Letter

Callose accumulation in specific phloem cell types reduces axillary bud growth in *Arabidopsis thaliana*

Shoot branching involves the coordinated regulation of the activity of meristems established in the axils of leaves along the stem (Mcsteen & Leyser, 2005). Once established, such axillary meristems often arrest as a dormant bud after the production of a few leaves. The hormone auxin, produced in the shoot apex, plays a central role in this process by moving downward in the stem and maintaining these axillary meristems in an inactive state, a process termed apical dominance (Snow, 1925, 1929; Morris, 1977). As auxin does not itself enter the buds, the auxin transport canalisation model for bud regulation was postulated (Li & Bangerth, 1999; Bennett *et al.*, 2006). According to this model, each bud, acting as an auxin source, must establish canalised auxin export to grow. The hormone self-reinforces its transport through positive feedback between flux and auxin transporter accumulation on the membrane of cells in the direction of flux (Sachs, 1969; Mitchison, 1980, 1981). Auxin largely relies on a series of active transporters, including the PIN-FORMED (PIN) family for its directional cell–cell movement (Gälweiler *et al.*, 1998; Bennett *et al.*, 2014). Depending on the relative strengths of the auxin sink in the stem and sources in the buds, and the level of feedback between auxin flux and transporter accumulation, some axillary buds might be able to activate while others would not (Prusinkiewicz *et al.*, 2009).

In parallel to the systemic action of auxin, the transcription factors BRANCHED 1 (BRC1) and, to a lesser degree, its close paralogue BRC2, regulate shoot branching by operating at a local level within buds. They negatively regulate bud activation (Aguilar-Martínez *et al.*, 2007) and act as signal integrators to adjust branching under a range of environmental conditions (Finlayson *et al.*, 2010; González-Grandío *et al.*, 2013; Seale *et al.*, 2017). Further regulators of shoot branching, such as strigolactone (SL) and cytokinin (CK) hormones appear to act by modulating auxin transport canalisation and *BRC1* expression. These hormones, unlike auxin, enter the bud directly from the stem, moving in the xylem transpiration stream (Domagalska & Leyser, 2011).

In addition to transmembrane transporters and flow in the lignified cells of the xylem, other regulators of bud growth could move via plasmodesmata (PD), the small channels connecting the cytoplasm of neighbouring plant cells (Li *et al.*, 2020). Long distance transport could also occur in the phloem, a specialised conduit for nutrients and signals (Turgeon & Wolf, 2009). Two phloem-mobile sugars, sucrose and trehalose 6-phosphate (Tre6P), have, for instance, been implicated in the control of shoot branching, as their levels increase in buds upon apex decapitation (Mason *et al.*, 2014; Fichtner *et al.*, 2017) and Arabidopsis plants with altered levels of Tre6P show distinct branching phenotypes (Fichtner *et al.*, 2021). Defoliation, removing the source of these compounds, or their exogenous application have opposing effects on bud growth (Mason *et al.*, 2014; Fichtner *et al.*, 2017). The role of these compounds is most likely to be a signalling, rather than metabolic, one as nonreadily assimilable sugars still elicit growth effects (Barbier *et al.*, 2015) and Tre6P is a known sucrose-specific signal in plants (Figueroa & Lunn, 2016). These metabolites can also influence PIN protein levels and *BRC1* expression (Mason *et al.*, 2014; Barbier *et al.*, 2015). The SL receptor DWARF 14 (D14) is another macromolecule present in the phloem sap of plants (Aki *et al.*, 2008; Batailler *et al.*, 2012) and its transport is necessary for tilling control in rice (Kameoka *et al.*, 2016).

Genetic tools to modulate long distance and local cell–cell connectivity are available in plants, one of the more widely used tools being the *icals3m* system. This tool, of which we make use in this study, consists of a mutant version of a *CALLOSE SYNTHASE 3 (CALS3)* gene, engineered under the control of an estrogen transactivator and tissue specific promoters. Callose is a polysaccharide lining PD and its accumulation due to the mutant, overactive, enzyme results in occlusion of PD in a temporally and spatially controlled manner (Vatén *et al.*, 2011).

The process of phloem unloading, the ultimate release of substances from this specialised conduit, has not been characterised in *Arabidopsis thaliana* buds. It could in principle occur symplastically (via PD) and/or apoplastically (via transporters) (Oparka, 1990). The *SUC2:GFP* reporter is a widely used tool to study symplastic unloading and is based on the *SUCROSE TRANSPORTER 2* promoter driving free GREEN FLUORESCENT PROTEIN (Imlau *et al.*, 1999). As the promoter is expressed in companion cells (CC) that load substances into the phloem sieve elements (Sauer & Stolz, 1994; Stadler & Sauer, 1996), GFP experiences long distance transport. It is only released in the presence of open PD connecting the phloem to surrounding cells (Imlau *et al.*, 1999; Stadler *et al.*, 2005a). It is conversely retained in the sieve elements in cases in which only apoplastic unloading occurs (Stadler *et al.*, 2005b; Werner *et al.*, 2011) as native transporters would not recognise GFP as a substrate for transport. When we imaged *SUC2:GFP* plants we observed a broad signal in sections across the inflorescence stem and its buds (Fig. 1a; Supporting information Fig. S1a), beyond the domain of *SUC2* expression (Fig. S1b). The result implied the existence of a symplastic domain in the inflorescence that could perform phloem unloading. The fluorescence pattern is also similar to that observed in Arabidopsis roots at the tip, where PD-driven unloading is observed as a diffuse GFP signal, while higher up in the root the signal is more restricted to the vasculature (in CCs and sieve elements) (Stadler *et al.*, 2005a) (Fig. S1c–e).

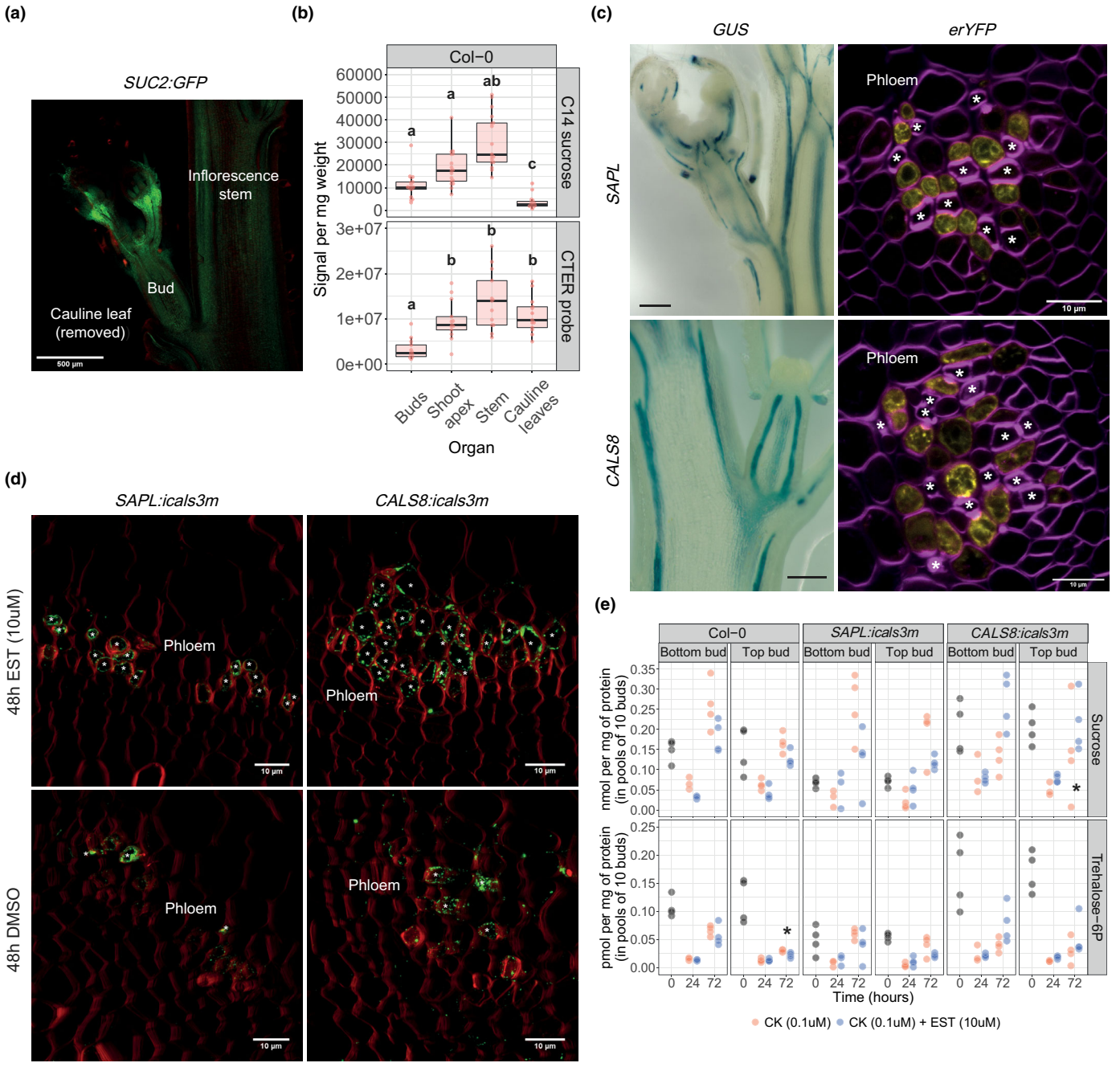

Fig. 1 Phloem unloading and phloem cell–cell connectivity in *Arabidopsis thaliana* inflorescence stems and buds. (a) *SUC2:GFP* signal in a longitudinal section of the inflorescence stem and one of its buds. GFP is rendered in green, propidium iodine stain is false coloured in red. (b) Radioactive ($n = 17$) or fluorescence ($n = 13$) signal intensity in inflorescence organs of plants supplied with label through the rosette leaves, scaled by fresh weight. Dots represent individual measurements, while the box plots provide median values (central horizontal bars), interquartile ranges (spaces between horizontal edges of the boxes) and extended ranges up to one and a half times the interquartile ranges, within spread of actual data points (vertical whiskers). Different letters indicate statistical differences in a Dunn's test with a *P*-value threshold of < 0.05. (c) *SAPL/CALS8:GUS* signal in the inflorescence and *SAPL/CALS8:erYFP* fluorescent signal in the phloem part of vascular bundles of the inflorescence stem. Yellow fluorescent protein (YFP) is rendered in yellow, while calcofluor white stain is false coloured in magenta. Asterisks indicate sieve element cells. (d) Callose immunolabelling in inflorescence stem sections from explants supplied with dimethyl sulfoxide (DMSO) or estradiol (EST) for 48 h. Signal from secondary antibody is rendered in green while calcofluor white stain is false coloured in red. *Indicates a cell with strong callose-related signal within the phloem. (e) Sucrose and trehalose-6P amounts at various time points after EST or noninductive treatment in buds of two-node explants with intact apices. Each dot represents a separate pool of buds. Black dots indicate timepoint 0, without any treatment. *Indicates statistically significant differences in a two-tailed Mann–Whitney test with a *P*-value threshold of <0.05. $n = 3$–4 per timepoint, genotype and treatment. Bar, 500 µm (a). Bars, 100 µm (c: GUS images); and 10 µm (c: YFP images and d).

To gain a quantitative appreciation of systemic delivery to the inflorescence we applied two tracers, 14C sucrose (Slewinski *et al.*, 2009) and the fluorescent phloem-mobile probe carboxytetraethylrhodamine – CTER (Knoblauch *et al.*, 2015) to rosette leaves of plants grown axenically just after floral transition. As mature leaves act as sources of photoassimilate for the plant (De Schepper *et al.*, 2013), in the labelled leaf ^{14}C sucrose would be recognised and loaded into the phloem by the native SUC2 transporter (Riesmeier *et al.*, 1994; Stadler & Sauer, 1996). CTER, conversely, is likely to enter the phloem nonselectively but be retained (and translocated) via ion-trapping mechanisms (Hsu & Kleier, 1996; Knoblauch *et al.*, 2015). Systemic transport in the xylem is unlikely as transpiration from the labelled leaf would oppose it. The inflorescence was dissected into its component parts (buds, shoot apex, stem and cauline leaves) 16 h later. Both tracers produced clear signals above background in all the organs of the inflorescence (Fig. S1f). The relative signals in the various organs (scaled by fresh weight and represented as percentage of total scaled signal) were largely equivalent between the two tracers with an exception in cauline leaves in which more fluorescent probe was observed than ^{14}C sucrose (Figs 1b, S1g,h). This might be due to *en-route* phloem-to-xylem transfer of the probe. Cauline leaves, which experience the highest transpiration rate among the tissues sampled, would then accumulate the extra signal. The presence of another phloem-mobile probe in xylem associated cells of sink tissues was indeed reported (Martins-Rodriguez, 2020). Although phloem-to-xylem sucrose transfer might also occur (Aubry *et al.*, 2019), CTER might more substantially leak or be less efficiently retrieved compared with sucrose. Overall, the inflorescence stem and the shoot apex seemed to be stronger sinks than the buds, at least when the latter are small and dormant. Delivery of CTER, which is unlikely to be taken up by endogenous transporters, provides further evidence that unloading in the inflorescence is, at least in part, symplastic. The PD of vascular tissues would therefore play key roles in the process.

To investigate the importance of vascular systemic and local transport we took advantage of two existing *icals3m* lines driven from root phloem specific promoters: the *SISTER OF APPLE (SAPL)* promoter, which is specific to CCs (plus meta sieve elements) and the *CALLOSE SYNTHASE 8 (CALS8)* promoter, which is expressed in phloem pole pericycle cells (Ross-Eliott *et al.*, 2017). The cell-type expression pattern seemed conserved in inflorescence stems, based on sections from reporter lines. GUS signals delineated patterns resembling vascular strands (Fig. 1c) and the *erYFP* signal was restricted to the phloem side of stem vascular bundles (Figs 1c, S2a,b). For *SAPL* the fluorescence signal was specifically associated with round cells smaller or of equal size to neighbouring sieve elements (the latter are identifiable by thick walls and associated strong calcofluor stain) while, for *CALS8*, fluorescence was observed in larger and more oblong-shaped cells next to the sieve elements (Figs 1c, S2a,b). These patterns, when compared with electron micrographs of the inflorescence phloem (Nintemann *et al.*, 2018) are compatible with *SAPL* expression in CCs and *CALS8* in (a potential subset of) phloem parenchyma cells. The pericycle, as an anatomical structure, is absent in above-ground tissues (Dubrovsky and Rost, 2001). However, as xylem pole pericycle-like cells have also been described in above-ground tissues (Sugimoto *et al.*, 2010), it is plausible that an equivalent domain exists in stems, raising interesting questions about its function.

The absence of *SAPL*-driven fluorescence in sieve elements, which contrasts previous reports (Ross-Eliott *et al.*, 2017), is most likely due to sieve elements being enucleate in the sections displayed. Sieve element expression, if any, would be restricted to areas more proximal to meristematic regions. To validate independently the patterns of the reporter constructs we interrogated a tissue and cell-type specific expression dataset of the inflorescence stem of Arabidopsis (Shi *et al.*, 2020). *SAPL* and *CALS8* transcripts were detected in phloem cell types (based on fluorescence-activated nuclear sorting) (Fig. S2c) and enriched in the phloem cap of vascular bundles (assessed using laser capture microdissection) (Fig. S2d). In those datasets, expression in other tissues, such as the epidermis (which we did not observe), was also reported (Fig. S2c). The promoters we used in the reporter constructs and in the *icals3m* constructs were the same, enabling correlations between the two in this study, regardless of potential additional native domains.

Excised inflorescence stem explants, carrying one or more nodes (each node consisting of a bud, its cauline leaf and associated stem segment), have been extensively used to study the process of shoot branching. They provide a simplified and tractable system in which bud growth can be monitored over several days with various treatments and manipulations (Ongaro *et al.*, 2008; Crawford *et al.*, 2010). The explants are placed in Eppendorf tubes sealed with Parafilm® (Methods S1) with the basal stem emersed in nutrient solution, to which relevant treatments can be added.

To determine whether induction of the *icals3m* constructs could be efficiently triggered in this experimental set-up, estradiol (EST), required to induce the constructs (Ross-Eliott *et al.*, 2017), was basally supplied in this way. This approach had previously successfully induced *BRC1* expression in buds (Seale *et al.*, 2017). We tested *CALS3* expression levels in the inflorescence stem following 24 h of induction. Normalised expression roughly doubled in *SAPL:icals3m* and *CALS8:icals3m* but not in Col-0 (Fig. S3a). We then assessed whether this transcriptional induction resulted in callose accumulation in the stem. In noninduced conditions the fluorescence signal from secondary antibodies raised against callose was generally restricted to individually spaced cells (Figs 1d, S3b). This signal is likely to correspond to mature sieve elements, which have high callose levels (Ross-Eliott *et al.*, 2017). A strong signal was instead observed in clusters of neighbouring cells 48 h after EST supply (Figs 1d, S3b). This callose accumulation was specific to the phloem part of the vascular bundles (Fig. S3b) and was consistent with the expression domains of *SAPL* or *CALS8* promoters (small or large cells neighbouring sieve elements – Fig. 1c). Therefore, EST can efficiently induce callose accumulation in the *SAPL* and *CALS8* expressing domains of inflorescence stem explants. These results laid the foundations for the study of potential physiological effects of this deposition.

In roots, induced callose accumulation in *CALS8:icals3m* (but not in *SAPL:icals3m*) results in blocked phloem unloading before and at 24 h (Ross-Eliott *et al.*, 2017). The reduced root growth rate of the *CALS8:icals3m* line upon induction (Ross-Eliott *et al.*, 2017) might be partially caused by impaired delivery of metabolites.

Altered systemic transport could be relevant in the context of bud growth as, for example, sucrose and Tre6P have been suggested to play roles in axillary bud activation and these substances may be delivered to growing buds via the phloem (Mason *et al.*, 2014; Fichtner *et al.*, 2017, 2021). To assess metabolite levels, axillary buds were collected from explants bearing two nodes and with intact apices at a 0 h timepoint and after 24 and 72 h of EST induction. CK was also supplied basally to the medium in which the explants were placed to enable bud escape from apical dominance and therefore bud activation (Muller *et al.*, 2015), probably via increased PIN3,4,7 levels in stem membranes (Waldie & Leyser, 2018) and downregulated *BRC1* levels (Braun *et al.*, 2012; Dun *et al.*, 2012; Seale *et al.*, 2017). Variation in sucrose and Tre6P levels (normalised by protein content) could be observed between genotypes, treatments and buds of the same explants (bottom vs top buds) (Fig. 1e). However, no consistent differences were observed between treatments. The magnitude of variation in the *icals3m* lines was similar to that of Col-0 (Fig. 1e), which is not responsive to EST. The same trends were also observed in a repeat in which top and bottom buds were pooled during collection (Fig. S4). These results indicated that sucrose and Tre6P levels were not affected in the *icals3m* lines employed, at time points when callose accumulation is visible in our sections. Phloem unloading to buds might not be blocked or buds might be able to modulate and buffer metabolite levels in the face of altered phloem delivery. In our hands it was not possible to perform phloem transport assays, of the type shown in Fig. 1b, in inflorescence explants.

To study if the induction of callose had physiological effects on axillary bud growth we employed both inflorescence explants with intact apices carrying one or two axillary buds and explants with decapitated apices and two buds (Fig. 2a,d,g,j). In the latter case bud activation is intrinsically induced by reduced competition for auxin export (Crawford et al 2010). In all the experiments, buds from the *SAPL:icals3m* line reached shorter final mean lengths upon EST supply (Fig. 2b,e,h,k). The differences were not always *statistically* significant but robustness to the claim was provided by the reproducibility of the pattern across experimental set-ups (Fig. 2a,d,g,j). When two buds were present (Fig. 2d–l), the effect was generally more visible in the one growing more strongly (longer bud), irrespective of its position on the explant (top vs bottom bud). Whether the top/bottom bud or both activate in two-node explants is not fully predictable, so we used a longer/shorter classification at the end of the time course. Traces for individual buds and plots showing relative growth biases between top and bottom buds are provided in Fig. S5a–g. The lack of growth changes in Col-0 supports the notion that EST is not generally detrimental to bud growth (Fig. 2a–i). Callose accumulation in the *CALS8:icals3m* line did not perturb bud growth dynamics (Fig. 2a–i), implying that this cellular domain might not carry relevance for the process being studied. The growth effect in *SAPL:icals3m* was not absolute or overwhelmingly strong and was more pronounced in explants bearing two buds. It is easier for buds to grow in a one-node systems, as competition occurs solely with the shoot apex, while in the two-node explants two apices of similar size compete with each other to establish rapid growth, making bud growth more sensitive to treatments (Crawford *et al.*, 2010).

To identify what processes might be altered in the *SAPL:icals3m* line, three metrics were extracted to describe bud growth dynamics (Methods S1). First, the percentage of explants with at least one active bud, determined using a 5-mm length threshold at the end of the time course, was largely unaffected in all genotypes upon EST supply and was mostly above 75% (below the inflorescence sketches in Fig. 2a,d,g,j). The approximate 10% variation observed does not correlate with EST treatment (Fig. 2a,d,g,j). Second, a proxy for the day of bud activation was calculated as the point of intersection of two linear regressions fitted to the growth curves of active buds (vertical bars in Figs 2b,c,e,f,h,i,k,l, S6a–d). This metric was also largely unaltered upon estradiol treatment in the genotypes tested. The third metric, the growth rate of the active buds, seemed reduced at late timepoints, around and after the calculated day of activation (Fig. 2c,f,i,l). This suggests that callose accumulation within the *SAPL* domain (but not in the *CALS8* domain) might influence postactivation bud growth dynamics rather than activation itself.

The *SAPL:icals3m* line was then crossed with the Arabidopsis branching mutants *d14* (Waters *et al*, 2012), *brc1* (Aguilar-Martínez *et al.*, 2007) and *pin3,pin4,pin7* (Bennett *et al.*, 2016). We employed two-node explants with intact apices to study if the construct's effects were modulated in these genetic backgrounds (Fig. 2j). Despite being prone to bud activation and growth (Bennett *et al.*, 2016; Seale *et al.*, 2017) *d14* and *brc1* mutants still displayed the reduced elongation upon *SAPL:icals3m* induction observed in a WT background (Fig. 2k,l). Growth was also generally restricted to the bottom bud in *d14* and *brc1* backgrounds (Fig. S5f,g). Conversely, EST did not seem to elicit strong effects in the *pin3,pin4,pin7* background (Fig. 2k,l). PIN proteins, which are known to be involved in bud activation, might therefore also play roles in the less studied process of postactivation growth. Interplay between cell–cell communication and hormonal networks have already been reported in other contexts (Paterlini, 2020).

Overall, the data presented here show that callose accumulation, within CC of the inflorescence, affects the growth of axillary buds via unknown mechanisms. In Arabidopsis, buds typically show paradormancy, with growth inhibition mainly imposed by signals associated with other organs on the plant rather than external clues (Lang *et al.*, 1987) and callose deposition seems specifically to influence postactivation bud growth dynamics. This is significantly different to the callose-dependent control of seasonal bud dormancy (and activation) in perennial plants (Rinne *et al.*, 2011; Tylewicz *et al.*, 2018; Singh *et al.*, 2019). Based on the extensive literature on the effects of *icals3m* constructs (Vatén *et al.*, 2011; Wu *et al.*, 2016; Liu *et al.*, 2017; Ross-Eliott *et al.*, 2017; Lai *et al.*, 2018; Miyashima *et al.*, 2019 as examples), we speculate that the growth rate reduction in *SAPL:icals3m* explants is due to impaired symplastic communication. The *SAPL* domain might be the source or the receiver of an unknown regulator that might need to be loaded/unloaded in CC during long distance transport or be trafficked locally. The *SAPL:icals3m* effects seem unrelated to early sugar levels in buds (preceding growth differences) and to the presence of the D14 protein, which are candidate phloem-mobile bud regulators (Mason *et al.*, 2014; Kameoka *et al.*, 2016; Fichtner *et al.*, 2017). However, the lack of direct evidence that callose accumulation in the inflorescence stem blocked cell–cell communication in the *SAPL*

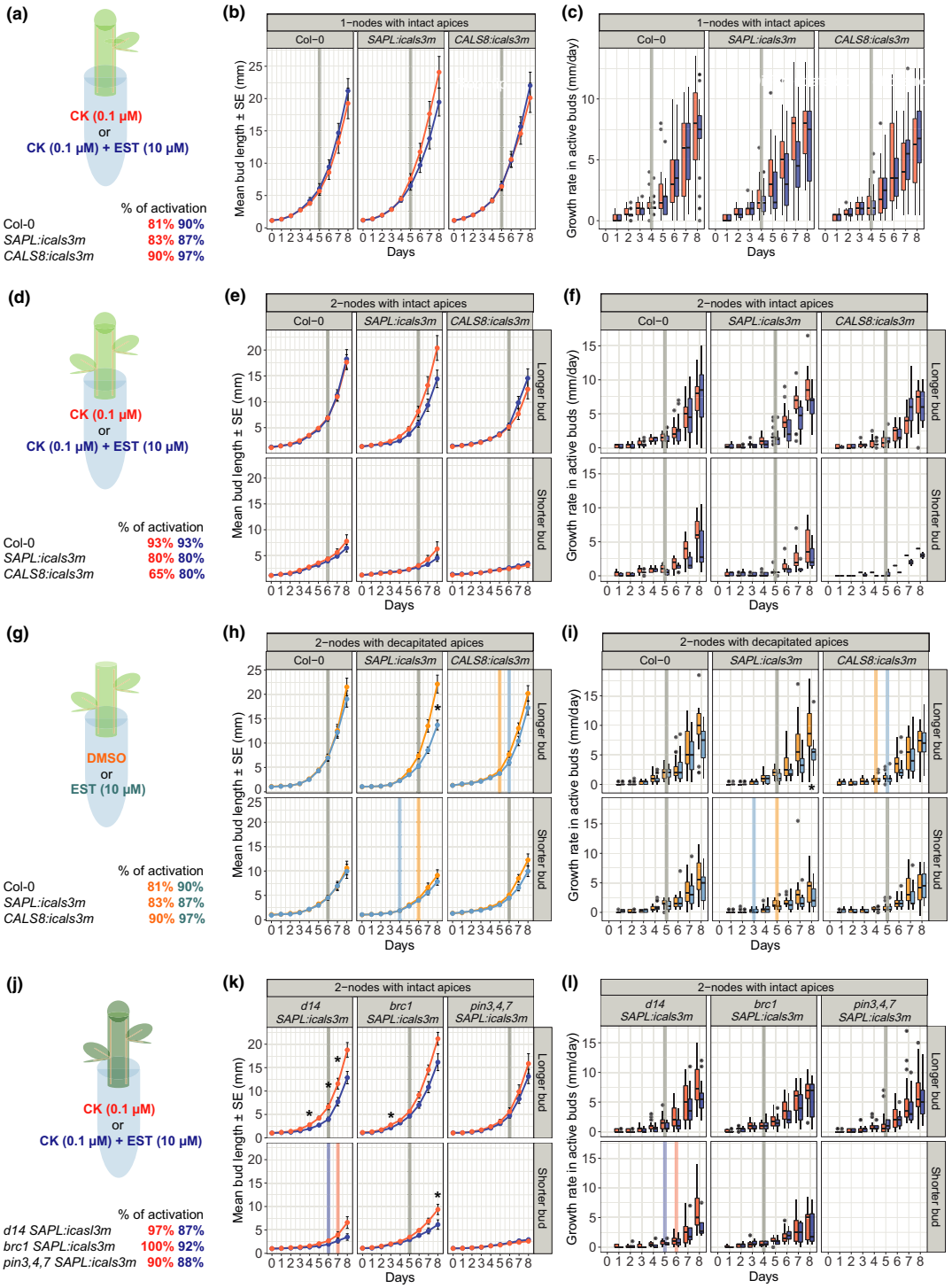

Fig. 2 Activation percentages, mean bud lengths, median days of activation and growth rates upon mock/callose induction in the *Arabidopsis thaliana* explant systems employed. (a–c) One-node explants. (d–f) Two-node explants with intact apices. (g–i) Two-node explants with decapitated apices. (j–l) Two-node explants from mutant genotypes with intact apices. Sketches of inflorescence explants and their activation percentages are shown in panels (a, d, g, j). Mean bud lengths (coloured dots) ± standard errors (SE) (black bars) are present in panels (b, e, h, k). Box plots for growth rates are shown in (c, f, i, l). Box plots provide median values (central horizontal bars), interquartile ranges (spaces between horizontal edges of the boxes) and extended ranges up to one and a half times the interquartile ranges, within spread of actual data points (vertical whiskers). Dots indicate values outside the whiskers' range. In the panels for bud lengths and growth rates vertical lines indicate the median day of activation of the buds in each treatment (rounded to the nearest day). If the bars overlap they are coloured in grey, otherwise they follow the colour scheme employed throughout the figure. *Indicates statistically significant differences in two-sided wilcox tests performed between treatments at each timepoint with a *P*-value threshold of <0.05. *P*-values, adjusted for multiple testing with false discovery rate (FDR). $n = 20–30$ for all treatments and genotypes.

(and *CALS8*) domains remains a limitation of this study. We were unable to robustly assess this due to the complexity of the plant material being employed. Nearly all other *icals3m* studies (involving imaging) to date have been performed in roots. Alternative scenarios must therefore be acknowledged here. For instance, the extensive callose deposition in the walls of *icals3m*-expressing cells (Fig. 1d) could also influence potential apoplastic signals. Sustained callose production could also become a competing sink for local metabolites, which might be particularly relevant during late rapid bud growth (when effects are visible in our assays) (Fig. 2a–l). This latter hypothesis, however, does not explain the lack of effects in the *CALS8:iclas3m* line. As previously mentioned, the metabolite analyses can be interpreted in multiple ways and do not provide definitive indications in terms of phloem unloading. Nonetheless, it is interesting that the *SAPL:icals3m* line, rather than the *CALS8:icals3m* line, displays phenotypic effects, the opposite to that observed in roots (Ross-Eliott *et al.*, 2017). A reversal of the importance of the respective cell types might be suggested.

Acknowledgements

We thank Jung-ok Heo and Sofia Otero (Sainsbury Laboratory – Cambridge) for providing *SAPL:erYFP* and *SUC2:erYFP* seeds, respectively. We acknowledge Firas Bou Daher and Matthieu Bourdon (Sainsbury Laboratory – Cambridge) for their advice and help with immunolocalisations. We thank Emmanuelle Bayer (Laboratoire de Biogenèse Membranaire – Bordeaux) for critical reading of the manuscript. This work was supported by the Gatsby Foundation (GAT3395/PR3 grant awarded to YH and GAT3272C to OL) and the Max Planck Society (FF).

Author contributions

AP, YH and OL designed the experiments, AP wrote the manuscript with input from all other authors. AP and RD generated plant lines. AP, DD and AV performed growth experiments. AP, and FF performed metabolite assays. MvR provided scripts for data analysis. All other experiments were performed by AP.

ORCID

Delfi Dorussen https://orcid.org/0000-0001-9808-588X
Franziska Fichtner https://orcid.org/0000-0002-4508-5437
Yrjö Helariutta https://orcid.org/0000-0002-7287-8459
Ottoline Leyser https://orcid.org/0000-0003-2161-3829
Andrea Paterlini https://orcid.org/0000-0002-1777-3160
Martin Rongen van https://orcid.org/0000-0002-1441-367X
Ana Vojnović https://orcid.org/0000-0003-1768-6320

Andrea Paterlini[1]*, Delfi Dorussen[1], Franziska Fichtner[2], Martin van Rongen[1], Ruth Delacruz[1], Ana Vojnović[1], Yrjö Helariutta[1,3] and Ottoline Leyser[1]*

[1]Sainsbury Laboratory, University of Cambridge, Cambridge, CB2 1LR, UK;
[2]Max Planck Institute of Molecular Plant Physiology, Potsdam-Golm 14476, Germany;
[3]Helsinki Institute of Life Science, University of Helsinki, Helsinki 00014, Finland
(*Authors for correspondence: emails andrea.paterlini@slcu.cam.ac.uk (AP) and ol235@cam.ac.uk (OL))

References

Aguilar-Martínez JA, Poza-Carrión C, Cubas P. 2007. Arabidopsis branched1 acts as an integrator of branching signals within axillary buds. *Plant Cell* **19**: 458–472.

Aki T, Shigyo M, Nakano R, Yoneyama T, Yanagisawa S. 2008. Nano scale proteomics revealed the presence of regulatory proteins including three ft-like proteins in phloem and xylem saps from rice. *Plant and Cell Physiology* **49**: 767–790.

Aubry E, Dinant S, Vilaine F, Bellini C, Le Hir R. 2019. Lateral transport of organic and inorganic solutes. *Plants* **8**: 20.

Barbier F, Péron T, Lecerf M, Perez-Garcia M-D, Barrière Q, Rolčík J, Boutet-Mercey S, Citerne S, Lemoine R, Porcheron B *et al.* 2015. Sucrose is an early modulator of the key hormonal mechanisms controlling bud outgrowth in *Rosa hybrida*. *Journal of Experimental Botany* **66**: 2569–2582.

Batailler B, Lemaitre T, Vilaine F, Sanchez C, Renard D, Cayla T, Beneteau J, Dinant S. 2012. Soluble and filamentous proteins in Arabidopsis sieve elements. *Plant, Cell & Environment* **35**: 1258–1273.

Bennett T, Brockington SF, Rothfels C, Graham SW, Stevenson D, Kutchan T, Rolf M, Thomas P, Wong GK-S, Leyser O *et al.* 2014. Paralogous radiations of pin proteins with multiple origins of noncanonical pin structure. *Molecular Biology and Evolution* **31**: 2042–2060.

Bennett T, Brockington SF, Rothfels C, Graham SW, Stevenson D, Kutchan T, Rolf M, Thomas P, Wong GK-S, Leyser O *et al.* 2014. Paralogous radiations of pin proteins with multiple origins of noncanonical pin structure. *Molecular Biology and Evolution* **31**: 2042–2060.

Bennett T, Hines G, van Rongen M, Waldie T, Sawchuk MG, Scarpella E, Ljung K, Leyser O. 2016. Connective auxin transport in the shoot facilitates communication between shoot apices. *PLoS Biology* **14**: e1002446.

Bennett T, Sieberer T, Willett B, Booker J, Luschnig C, Leyser O. 2006. The Arabidopsis MAX pathway controls shoot branching by regulating auxin transport. *Current Biology* **16**: 553–563.

Braun N, de Saint Germain A, Pillot J-P, Boutet-Mercey S, Dalmais M, Antoniadi I, Li X, Maia-Grondard A, Le Signor C, Bouteiller N *et al.* 2012. The pea tcp transcription factor PsBRC1 acts downstream of strigolactones to control shoot branching. *Plant Physiology* **158**: 225–238.

Crawford S, Shinohara N, Sieberer T, Williamson L, George G, Hepworth J, Müller D, Domagalska MA, Leyser O. 2010. Strigolactones enhance competition between shoot branches by dampening auxin transport. *Development* **137**: 2905–2913.

Domagalska MA, Leyser O. 2011. Signal integration in the control of shoot branching. *Nature Reviews Molecular Cell Biology* **12**: 211–221.

Dubrovsky JG, Rost TL. 2001. *Pericycle. eLS.* Wiley and Sons.

Dun EA, de Saint GA, Rameau C, Beveridge CA. 2012. Antagonistic action of strigolactone and cytokinin in bud outgrowth control. *Plant Physiology* **158**: 487–498.

Fichtner F, Barbier FF, Feil R, Watanabe M, Annunziata MG, Chabikwa TG, Höfgen R, Stitt M, Beveridge CA, Lunn JE. 2017. Trehalose 6-phosphate is involved in triggering axillary bud outgrowth in garden pea (*Pisum sativum* L.). *The Plant Journal* **92**: 611–623.

Fichtner F, Barbier FF, Annunziata MG, Feil R, Olas JJ, Mueller-Roeber B, Stitt M, Beveridge CA, Lunn JE. 2021. Regulation of shoot branching in Arabidopsis by trehalose 6-phosphate. *New Phytologist* **229**: 2135–2151.

Figueroa CM, Lunn JE. 2016. A tale of two sugars: trehalose 6-phosphate and sucrose. *Plant Physiology* **172**: 7–27.

Finlayson SA, Krishnareddy SR, Kebrom TH, Casal JJ. 2010. Phytochrome regulation of branching in Arabidopsis. *Plant Physiology* **152**: 1914–1927.

Gälweiler L, Guan C, Müller A, Wisman E, Mendgen K, Yephremov A, Palme K. 1998. Regulation of polar auxin transport by atpin1 in Arabidopsis vascular tissue. *Science* **282**: 2226–2230.

González-Grandío E, Poza-Carrión C, Sorzano COS, Cubas P. 2013. Branched1 promotes axillary bud dormancy in response to shade in Arabidopsis. *Plant Cell* **25**: 834–850.

Hsu FC, Kleier DA. 1996. Phloem mobility of xenobiotics VIII. A short review. *Journal of Experimental Botany* **47**: 1265–1271.

Imlau A, Truernit E, Sauer N. 1999. Cell-to-cell and long-distance trafficking of the green fluorescent protein in the phloem and symplastic unloading of the protein into sink tissues. *Plant Cell* **11**: 309–322.

Kameoka H, Dun EA, Lopez-Obando M, Brewer PB, de Saint GA, Rameau C, Beveridge CA, Kyozuka J. 2016. Phloem transport of the receptor dwarf14 protein is required for full function of strigolactones. *Plant Physiology* **172**: 1844–1852.

Knoblauch M, Vendrell M, De Leau E, Paterlini A, Knox K, Ross-Elliot T, Reinders A, Brockman SA, Ward J, Oparka K. 2015. Multispectral phloem-mobile probes: properties and applications. *Plant Physiology* **167**: 1211–1220.

Lang G, Early J, Martin G, Darnell R. 1987. Endo-, para-, and ecodormancy: physiological terminology and classification for dormancy research. *HortScience* **22**: 371–377.

Li C-J, Bangerth F. 1999. Autoinhibition of indoleacetic acid transport in the shoots of two-branched pea (*Pisum sativum*) plants and its relationship to correlative dominance. *Physiologia Plantarum* **106**: 415–420.

Li ZP, Paterlini A, Glavier M, Bayer EM. 2020. Intercellular trafficking via plasmodesmata: molecular layers of complexity. *Cellular and Molecular Life Sciences* **78**: 799–816.

Mason MG, Ross JJ, Babst BA, Wienclaw BN, Beveridge CA. 2014. Sugar demand, not auxin, is the initial regulator of apical dominance. *Proceedings of the National Academy of Sciences, USA* **111**: 6092–6097.

McSteen P, Leyser O. 2005. Shoot branching. *Annual Review of Plant Biology* **56**: 353–374.

Mitchison G. 1980. A model for vein formation in higher plants. *Proceedings of the Royal Society of London. Series B. Biological Sciences* **207**: 79–109.

Mitchison G. 1981. The polar transport of auxin and vein patterns in plants. *Philosophical Transactions of the Royal Society of London. B, Biological Sciences* **295**: 461–471.

Morris D. 1977. Transport of exogenous auxin in two-branched dwarf pea seedlings (*Pisum sativum* L.). *Planta* **136**: 91–96.

Müller D, Waldie T, Miyawaki K, To JP, Melnyk CW, Kieber JJ, Kakimoto T, Leyser O. 2015. Cytokinin is required for escape but not release from auxin mediated apical dominance. *The Plant Journal* **82**: 874–886.

Nintemann SJ, Hunziker P, Andersen TG, Schulz A, Burow M, Halkier BA. 2018. Localization of the glucosinolate biosynthetic enzymes reveals distinct spatial patterns for the biosynthesis of indole and aliphatic glucosinolates. *Physiologia Plantarum* **163**: 138–154.

Ongaro V, Bainbridge K, Williamson L, Leyser O. 2008. Interactions between axillary branches of Arabidopsis. *Molecular Plant* **1**: 388–400.

Oparka KJ. 1990. What is phloem unloading? *Plant Physiology* **94**: 393–396.

Paterlini A. 2020. Uncharted routes: exploring the relevance of auxin movement via plasmodesmata. *Biology Open* **9**: bio055541.

Prusinkiewicz P, Crawford S, Smith RS, Ljung K, Bennett T, Ongaro V, Leyser O. 2009. Control of bud activation by an auxin transport switch. *Proceedings of the National Academy of Sciences, USA* **106**: 17431–17436.

Riesmeier JW, Willmitzer L, Frommer WB. 1994. Evidence for an essential role of the sucrose transporter in phloem loading and assimilate partitioning. *EMBO Journal* **13**: 1–7.

Rinne PL, Welling A, Vahala J, Ripel L, Ruonala R, Kangasjärvi J, van der Schoot C. 2011. Chilling of dormant buds hyperinduces flowering locus t and recruits ga-inducible 1, 3-β-glucanases to reopen signal conduits and release dormancy in populus. *Plant Cell* **23**: 130–146.

Rodrigues CM, Müdsam C, Keller I, Zierer W, Czarnecki O, Corral JM, Reinhardt F, Nieberl P, Fiedler-Wiechers K, Sommer F *et al.* 2020. Vernalization alters sink and source identities and reverses phloem translocation from taproots to shoots in sugar beet. *Plant Cell* **32**: 3206–3223.

Ross-Elliott TJ, Jensen KH, Haaning KS, Wager BM, Knoblauch J, Howell AH, Mullendore DL, Monteith AG, Paultre D, Yan D *et al.* 2017. Phloem unloading in Arabidopsis roots is convective and regulated by the phloem-pole pericycle. *Elife* **6**: e24125.

Sachs T. 1969. Polarity and the induction of organized vascular tissues. *Annals of Botany* **33**: 263–275.

Sauer N, Stolz J. 1994. SUC1 and SUC2: two sucrose transporters from Arabidopsis thaliana; expression and characterization in baker's yeast and identification of the histidine-tagged protein. *The Plant Journal* **6**: 67–77.

De Schepper V, De Swaef T, Bauweraerts I, Steppe K. 2013. Phloem transport: a review of mechanisms and controls. *Journal of Experimental Botany* **64**: 4839–4850.

Seale M, Bennett T, Leyser O. 2017. Brc1 expression regulates bud activation potential but is not necessary or sufficient for bud growth inhibition in Arabidopsis. *Development* **144**: 1661–1673.

Shi D, Jouannet V, Agustí J, Kaul V, Levitsky V, Sanchez P, Mironova VV, Greb T. 2020. Tissue-specific transcriptome profiling of the Arabidopsis inflorescence stem reveals local cellular signatures. *Plant Cell* **33**: 200–223.

Singh RK, Miskolczi P, Maurya JP, Bhalerao RP. 2019. A tree ortholog of short vegetative phase floral repressor mediates photoperiodic control of bud dormancy. *Current Biology* **29**: 128–133.

Slewinski TL, Meeley R, Braun DM. 2009. Sucrose transporter1 functions in phloem loading in maize leaves. *Journal of Experimental Botany* **60**: 881–892.

Snow R. 1925. The correlative inhibition of the growth of axillary buds. *Annals of Botany* **39**: 841–859.

Snow R. 1929. The young leaf as the inhibiting organ. *New Phytologist* **28**: 345–358.

Stadler R, Lauterbach C, Sauer N. 2005b. Cell-to-cell movement of green fluorescent protein reveals post-phloem transport in the outer integument and identifies symplastic domains in Arabidopsis seeds and embryos. *Plant Physiology* **139**: 701–712.

Stadler R, Sauer N. 1996. The Arabidopsis thaliana *AtSUC2* gene is specifically expressed in companion cells. *Botanica Acta* **109**: 299–306.

Stadler R, Wright KM, Lauterbach C, Amon G, Gahrtz M, Feuerstein A, Oparka KJ, Sauer N. 2005a. Expression of gfp-fusions in Arabidopsis companion cells reveals non-specific protein trafficking into sieve elements and identifies a novel post-phloem domain in roots. *The Plant Journal* **41**: 319–331.

Sugimoto K, Jiao Y, Meyerowitz EM. 2010. Arabidopsis regeneration from multiple tissues occurs via a root development pathway. *Developmental Cell* **18**: 463–471.

Turgeon R, Wolf S. 2009. Phloem transport: cellular pathways and molecular trafficking. *Annual Review of Plant Biology* **60**: 207–221.

Tylewicz S, Petterle A, Marttila S, Miskolczi P, Azeez A, Singh RK, Immanen J, Mähler N, Hvidsten TR, Eklund DM *et al.* 2018. Photoperiodic control of seasonal growth is mediated by aba acting on cell-cell communication. *Science* **360**: 212–215.

Vatén A, Dettmer J, Wu S, Stierhof Y-D, Miyashima S, Yadav S, Roberts C, Campilho A, Bulone V, Lichtenberger R *et al.* 2011. Callose biosynthesis regulates symplastic trafficking during root development. *Developmental Cell* **21**: 1144–1155.

Waldie T, Leyser O. 2018. Cytokinin targets auxin transport to promote shoot branching. *Plant Physiology* **177**: 803–818.

Waters MT, Nelson DC, Scaffidi A, Flematti GR, Sun YK, Dixon KW, Smith SM. 2012. Specialisation within the dwarf14 protein family confers distinct responses to karrikins and strigolactones in Arabidopsis. *Development* **139**: 1285–1295.

Werner D, Gerlitz N, Stadler R. 2011. A dual switch in phloem unloading during ovule development in Arabidopsis. *Protoplasma* **248**: 225–235.

Supporting Information

Additional Supporting Information may be found online in the Supporting Information section at the end of the article.

Fig. S1 Phloem unloading into inflorescence stems and their organs.

Fig. S2 Expression domains of *SAPL* and *CALS8* promoters.

Fig. S3 Induction of *SAPL:icals3m* and *CALS8:icals3m* constructs in inflorescence explants.

Fig. S4 Metabolite levels in buds of two-node explants with intact apices.

Fig. S5 Individual growth traces of Col-0, *SAPL:icals3m* and *CALS8:icals3m* buds upon EST or noninductive treatments and bottom-top bud relative growth biases in two-node explants.

Fig. S6 Day of activation in Col-0, *SAPL:icals3m* and *CALS8:icals3m* inflorescence explants upon EST or noninductive treatment.

Methods S1 Supplementary methods.

Please note: Wiley Blackwell are not responsible for the content or functionality of any Supporting Information supplied by the authors. Any queries (other than missing material) should be directed to the *New Phytologist* Central Office.

Key words: buds, callose, companion cells, phloem, plasmodesmata, shoot branching.

Received, 28 December 2020; accepted, 10 April 2021.